

# Norepinephrine triggers release of glial ATP to increase postsynaptic efficacy

Grant R J Gordon<sup>1</sup>, Dinara V Baimoukhametova<sup>1</sup>, Sarah A Hewitt<sup>1</sup>, W R A Kosala J S Rajapaksha<sup>2</sup>, Thomas E Fisher<sup>2</sup> & Jaideep S Bains<sup>1</sup>

Glial cells actively participate in synaptic transmission. They clear molecules from the synaptic cleft, receive signals from neurons and, in turn, release molecules that can modulate signaling between neuronal elements. Whether glial-derived transmitters can contribute to enduring changes in postsynaptic efficacy, however, remains to be established. In rat hypothalamic paraventricular nucleus, we demonstrate an increase in the amplitude of miniature excitatory postsynaptic currents in response to norepinephrine that requires the release of ATP from glial cells. The increase in quantal efficacy, which likely results from an insertion of AMPA receptors, is secondary to the activation of P2X<sub>7</sub> receptors, an increase in postsynaptic calcium and the activation of phosphatidylinositol 3-kinase. The gliotransmitter ATP, therefore, contributes directly to the regulation of postsynaptic efficacy at glutamatergic synapses in the CNS.

Astrocytes<sup>1–4</sup> and Schwann cells<sup>5</sup> can respond to and influence neuronal signals by releasing glial-derived substances (gliotransmitters). However, until very recently<sup>3</sup>, the most ubiquitous gliotransmitter, ATP, had been categorized almost exclusively as a paracrine messenger responsible for inter-glial propagation of calcium waves<sup>6–8</sup>. There is now growing support for the idea that activation of neuronal purinergic receptors can affect synaptic plasticity<sup>9–11</sup>. Until now, the majority of the characterized actions of ATP on excitatory synaptic transmission, however, have been short-term, presynaptic changes in neurotransmitter release, with little evidence for enduring, postsynaptic changes. Given that ATP-gated P2X channels are calcium permeable<sup>12</sup> and that the P2X<sub>7</sub> receptor is linked directly to phosphatidylinositol 3-kinase (PI3K)<sup>13</sup>, an intracellular signaling molecule that is crucial for the insertion of AMPA receptors<sup>14</sup> and the expression of LTP in the hippocampus<sup>15,16</sup> and amygdala<sup>17</sup>, it seems plausible to hypothesize that ATP can induce enduring changes in postsynaptic efficacy.

To study the putative contributions of glial-derived ATP to postsynaptic changes in synaptic strength, we examined glutamatergic synapses onto magnocellular neurosecretory cells (MNCs) in the paraventricular nucleus (PVN). The glial cells that surround the MNCs and their synaptic contacts show a notable degree of anatomical plasticity. In response to physiological challenges, they undergo a remodeling process that results in a decrease in the astrocytic coverage of synaptic contacts<sup>18,19</sup>. Taking advantage of this propensity of glial cells to retract when the animal is physiologically challenged, we can study synaptic function during conditions in which there is either a relative paucity or relative abundance of glial cells surrounding the

MNCs. This allows us to address directly the question of glia and, by extension, gliotransmitters in the regulation of synaptic function. Important for the study of ATP and long-term synaptic plasticity in this system is the demonstration that the MNCs have several subtypes of P2X receptors that are permeable to calcium<sup>12</sup>, the critical trigger for enduring changes in postsynaptic efficacy<sup>20</sup>. Furthermore, ATP receptors are critical for the increases in activity observed in MNCs in response to physiological perturbations that selectively recruit noradrenergic fibers<sup>21</sup> and for facilitating hormone release in response to norepinephrine<sup>22</sup>. As a large fraction of catecholaminergic (and, more specifically, noradrenergic) terminals in the brain lack postsynaptic contacts<sup>23</sup>, this raises the possibility that signaling in this vital homeostatic circuit may require dynamic glial-neuronal interactions.

Here, we demonstrate that norepinephrine increases the amplitude of miniature excitatory postsynaptic currents (mEPSCs) in MNCs through the release of ATP from glial cells. ATP acts at postsynaptic P2X<sub>7</sub> receptors to promote the insertion of AMPA receptors through a mechanism requiring the calcium-dependent activation of PI3K. These data demonstrate a new mechanism by which glial cells can affect synaptic strength at excitatory synapses.

## RESULTS

We examined changes in mEPSC amplitude as a measure of synaptic strength because of the compelling evidence that mEPSCs are important for information transfer in a number of vertebrate preparations<sup>24–26</sup>. Changes in mEPSC amplitude directly translate into changes in the firing patterns of CNS neurons, and, in particular, the MNCs<sup>27</sup>.

<sup>1</sup>Hotchkiss Brain Institute and the Department of Physiology and Biophysics, University of Calgary, 3330 Hospital Drive NW, Calgary, Alberta, Canada T2N 4N1.

<sup>2</sup>Department of Physiology, College of Medicine, University of Saskatchewan, 107 Wiggins Road, Saskatoon, Saskatchewan, Canada S7N 5E5. Correspondence should be addressed to J.B. (jsbains@ucalgary.ca).

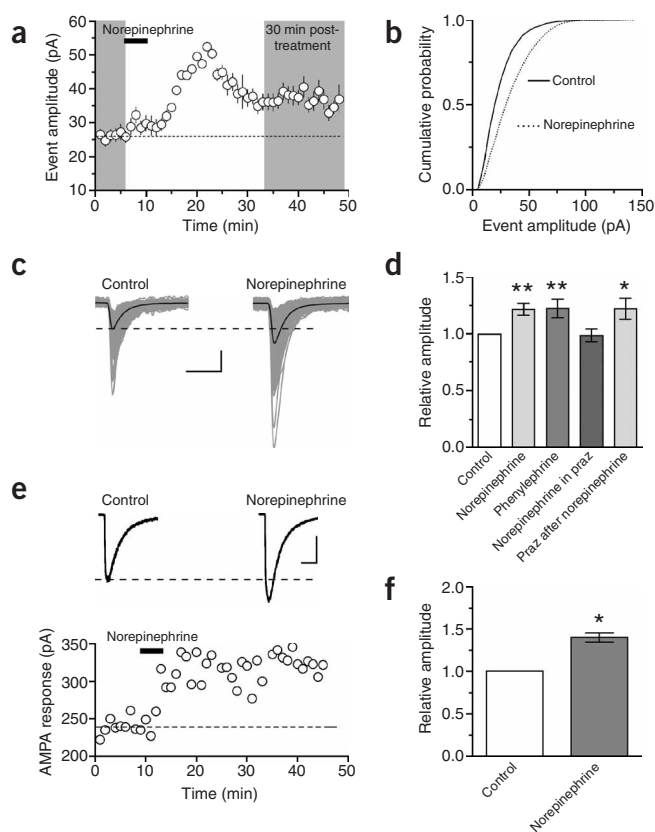


**Figure 1** Norepinephrine induces an enduring increase in mEPSC amplitude that is accompanied by an increase in postsynaptic efficacy. **(a)** Running average of mEPSC amplitudes in 1-min bins. Norepinephrine was bath applied for 5 min (200  $\mu$ M). Amplitude values were assessed at the time points indicated by gray bands. **(b)** Cumulative fraction plot of mEPSC amplitudes from the control condition and 30 min after norepinephrine treatment ( $P < 0.01$ ). **(c)** Average (black) and raw (gray) mEPSC traces from the same time points as described in **a** and **b**. **(d)** Summary showing the enduring increase in mEPSC amplitude observed after application of norepinephrine ( $1.22 \pm 0.05$ ,  $P < 0.01$ ,  $n = 20$ ), phenylephrine ( $1.23 \pm 0.08$ ,  $P < 0.01$ ,  $n = 5$ ), norepinephrine in prazosin ( $0.99 \pm 0.05$ ,  $P > 0.05$ ,  $n = 6$ ) and prazosin after norepinephrine ( $1.22 \pm 0.09$ ,  $P < 0.05$ ,  $n = 4$ ). **(e)** Postsynaptic responses to focal AMPA puff; average traces from control condition and 30 min post-norepinephrine shown above graph. **(f)** Summary showing an increase in postsynaptic responsiveness to AMPA puff 30 min post-norepinephrine ( $1.41 \pm 0.09$ ,  $P < 0.05$ ,  $n = 5$ ). Scale bars, **a**: 20 pA, 5 ms; **e**: 100 pA, 250 ms. Error bars: s.e.m. \*,  $P < 0.05$ ; \*\*,  $P < 0.01$ , here and in all figures.

we investigated whether norepinephrine increased the postsynaptic response to exogenous AMPA application. The response to focal application of AMPA (see Methods) directly onto MNCs (mean:  $197.4 \pm 28.9$  pA) was significantly increased after norepinephrine application ( $1.41 \pm 0.09$ ,  $P < 0.05$ ,  $n = 5$ ; **Fig. 1e,f**).

### Norepinephrine triggers AMPA receptor insertion

We used peak-scaled non-stationary noise analysis (PSNA)<sup>32</sup> to investigate whether the increase in synaptic strength was associated with an increase in AMPA channel conductance<sup>33</sup>. To ensure that the fluctuation in mEPSC decay arose mostly from stochastic channel properties, we examined mEPSCs in the control condition and after norepinephrine treatment and confirmed there was no strong relationship between the rise time and decay time of the mEPSCs<sup>32</sup> (control: 10–90 rise-time versus decay-time  $r^2 = 0.15 \pm 0.02$ ; 30 min post-norepinephrine treatment: 10–90 rise-time versus decay-time  $r^2 = 0.11 \pm 0.03$ ,  $P > 0.05$ ,  $n = 6$ ). To establish that PSNA yielded unitary currents that were linearly related to voltage and predicted the reversal potential of the channel (approximately 0 mV), cells were voltage clamped at different potentials, and unitary current values satisfying these criteria were obtained (–40 mV:  $-1.73 \pm 0.29$  pA; –60 mV:  $-2.61 \pm 0.39$  pA; –80 mV:  $-3.32 \pm 0.44$  pA; channel reversal: 4.4 mV,  $n = 5$ ; **Fig. 2a,b**). Next, we determined that there was no change in the unitary AMPA conductance upon application of a low dose of the AMPA receptor blocker DNQX (500 nM); this decreases mEPSC amplitude by completely blocking a fraction of AMPA receptors (control:  $16.82 \pm 2.85$  pS; DNQX:  $16.35 \pm 2.81$  pS,  $P > 0.05$ ,  $n = 6$ ; **Fig. 2c,d**). The mEPSC amplitude in DNQX was  $0.73 \pm 0.08$ ,  $P < 0.05$ ,  $n = 7$ . The unitary conductance of mEPSCs in the control condition was not different from that after norepinephrine (control:  $20.02 \pm 3.63$  pS; post-norepinephrine:  $18.22 \pm 2.69$  pS,  $P > 0.05$ ,  $n = 7$ ; **Fig. 2e,f**). These values are consistent with those reported previously for excitatory synapses onto MNCs in the supraoptic nucleus (SON) of the hypothalamus<sup>34</sup>.

It is widely accepted that the insertion of postsynaptic AMPA receptors is a mechanism by which synapses increase their strength<sup>20</sup>. We tested for this possibility by targeting SNARE-dependent vesicle exocytosis. Inclusion in our patch pipette of botulinum toxin C (5  $\mu$ g/ml), which proteolytically cleaves the tSNARE syntaxin<sup>35</sup>, completely blocked the enduring increase in quantal amplitude caused by norepinephrine ( $0.96 \pm 0.04$ ,  $P > 0.05$ ,  $n = 7$ ; **Fig. 3a**). Consistent with previous observations<sup>20</sup>, we found that this exocytotic process requires increases in postsynaptic calcium, as the inclusion of EGTA (10 mM) in

### Norepinephrine permanently increases mEPSC amplitude

Bath application of norepinephrine (5 min, 200  $\mu$ M) elicited three sequential changes in mEPSC amplitude. These were, in temporal order, a small enhancement followed by a robust increase lasting approximately 15 min, which in turn relaxed to a new mean and remained elevated even during our longest whole-cell recordings (which exceeded 90 min in length). This manuscript focuses on the enduring increase in mEPSC amplitude and not the initial increases during agonist application. In each cell, control mEPSC amplitudes were compared with those 30 min after treatment (gray demarcations in **Fig. 1a**). A minimum 5-min recording segment was used for the analysis. The enduring increase in mEPSC amplitude was  $1.22 \pm 0.05$  ( $P < 0.01$ ,  $n = 20$ ; **Fig. 1a–d**); all values are expressed as a fraction or multiple of the control condition. For the remainder of the manuscript, we often use the terms ‘increase in synaptic strength’ or ‘synaptic potentiation’ interchangeably with ‘enduring increase in mEPSC amplitude’.

The  $\alpha_1$  adrenoceptor mediates the excitatory effects of norepinephrine on MNCs<sup>28–31</sup>. Here, the  $\alpha_1$ -adrenoceptor agonist phenylephrine (5 min, 200  $\mu$ M) effectively mimicked the effects of norepinephrine ( $1.23 \pm 0.08$ ,  $P < 0.01$ ,  $n = 5$ ; **Fig. 1d**), whereas the  $\alpha_1$ -adrenoceptor antagonist prazosin (10  $\mu$ M) attenuated them ( $0.99 \pm 0.05$ ,  $P > 0.05$ ,  $n = 6$ ; **Fig. 1d**). To rule out the possibility that the enduring increase in synaptic strength resulted from a slow washout of the agonist, prazosin was added to the bath immediately after norepinephrine application was terminated. This did not attenuate the enduring increase in synaptic strength ( $1.22 \pm 0.09$ ,  $P < 0.05$ ,  $n = 4$ , **Fig. 1d**). These data collectively suggest that transient activation of  $\alpha_1$ -adrenoceptors triggers a robust and enduring enhancement of mEPSC amplitude.

This increase in synaptic strength is reminiscent of activity-dependent changes in postsynaptic receptor function responsible for long-term potentiation (LTP) at cortical synapses<sup>20</sup>. Consequently,

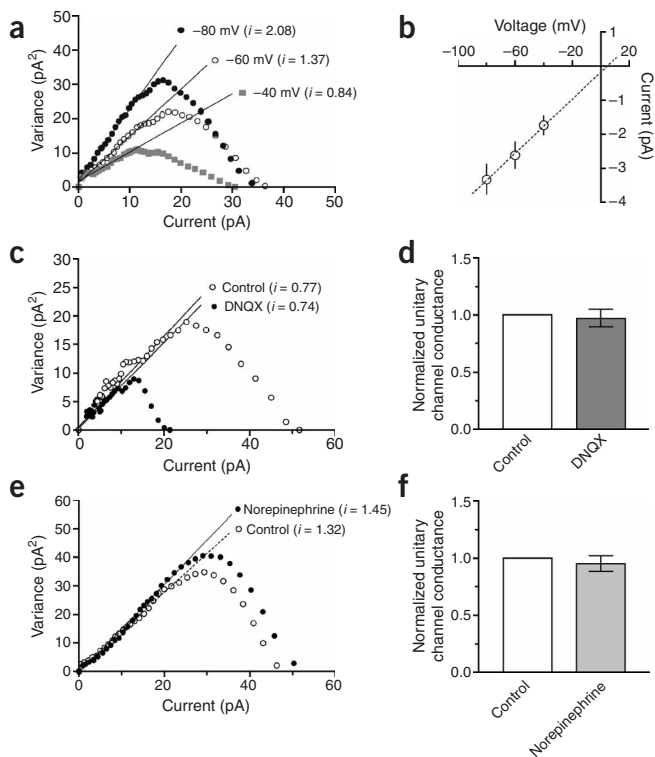


**Figure 2** The enduring increase in mEPSC amplitude is not associated with an increase in AMPA channel conductance. **(a)** Variance versus current for mEPSCs when the postsynaptic cell is held at different potentials. The slope,  $i$ , represents the unitary channel current. **(b)** The unitary AMPA channel current changes linearly with voltage and estimates the reversal potential of the channel ( $-40$  mV:  $-1.73 \pm 0.29$  pA,  $-60$  mV:  $-2.61 \pm 0.39$  pA,  $-80$  mV:  $-3.32 \pm 0.44$  pA, channel reversal:  $4.4$  mV,  $n = 5$ ). **(c)** There is no change in the unitary AMPA channel current between control mEPSCs and mEPSCs treated with DNQX ( $500$  nM). **(d)** Summary of effects of DNQX on channel conductance ( $0.97 \pm 0.07$ ,  $P > 0.05$ ,  $n = 6$ ). **(e)** There is no change in the unitary AMPA channel current between control mEPSCs and mEPSCs post-norepinephrine. **(f)** Summary of effects of norepinephrine on channel conductance ( $0.95 \pm 0.06$ ,  $P > 0.05$ ,  $n = 7$ ). Error bars: s.e.m.

our internal solution completely blocked the effects of norepinephrine ( $1.03 \pm 0.02$ ,  $P > 0.05$ ,  $n = 6$ , **Fig. 3b**). Finally, we examined the cellular signals required for the insertion of AMPA receptors by targeting PI3K, which is important in the expression of LTP in the hippocampus<sup>14–16</sup>. Inclusion of either of two different PI3K inhibitors in the patch pipette (wortmannin ( $100$  nM) or LY294002 ( $10$   $\mu$ M)) blocked the effects of norepinephrine on mEPSC amplitude (wortmannin:  $1.02 \pm 0.02$ ,  $P > 0.05$ ,  $n = 4$ ; LY294002:  $1.01 \pm 0.02$ ,  $P > 0.05$ ,  $n = 5$ , **Fig. 3c**). Collectively, these data suggest that norepinephrine promotes the calcium-dependent, postsynaptic insertion of AMPA receptors through the activation of PI3K.

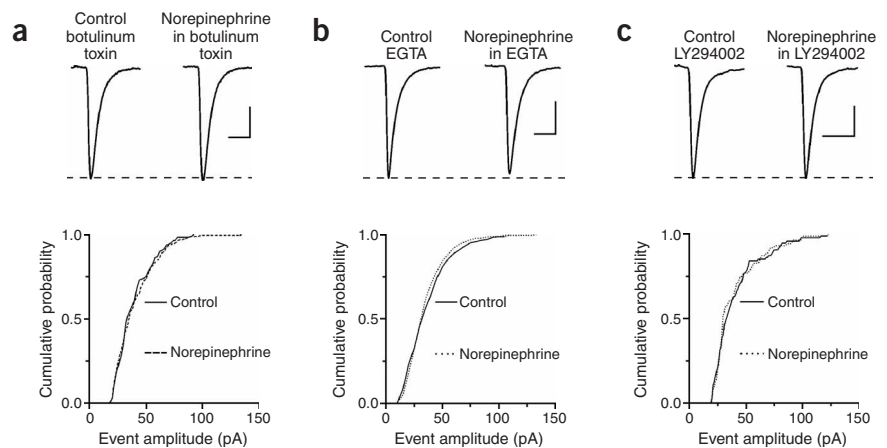
### Norepinephrine does not use postsynaptic receptors

To examine the possibility that activation of the postsynaptic  $G_q$ -coupled  $\alpha_1$ -adrenoceptor directly increases mEPSC amplitude, we targeted two separate points on the  $\alpha_1$ -adrenoceptor intracellular

cascade. First, we introduced thapsigargin ( $5$   $\mu$ M), which depletes calcium stores, into our patch electrode. This treatment did not block the norepinephrine-mediated increase in quantal amplitude ( $1.22 \pm 0.05$ ,  $P < 0.01$ ,  $n = 8$ , **Fig. 4a**). Second, we targeted the  $G_q$ -protein directly with intracellular perfusion of GDP- $\beta$ s ( $1$  mM). This experimental manipulation had no impact on the enduring increase in mEPSC amplitude after norepinephrine treatment ( $1.19 \pm 0.02$ ,  $P < 0.01$ ,  $n = 6$ , **Fig. 4b**). To confirm the validity of this negative result, we conducted an additional experiment in which we bath applied the glucocorticoid receptor agonist, dexamethasone ( $50$   $\mu$ M,  $3$  min). Activation of postsynaptic glucocorticoid receptors decreases glutamate release through a mechanism that requires the production of endocannabinoids<sup>36</sup>. Consistent with this report, dexamethasone decreased mEPSC frequency ( $0.49 \pm 0.04$ ,  $P < 0.01$  compared with control condition,  $n = 3$ ). This was attenuated when GDP- $\beta$ s was included in the internal solution ( $0.86 \pm 0.13$ ,  $P < 0.05$  compared with dexamethasone alone,  $n = 3$ ). Collectively, these data suggest that postsynaptic  $\alpha_1$ -adrenoceptors are not responsible for the enduring increase in mEPSC amplitude.

We have previously shown that norepinephrine transiently increases the frequency of glutamate release through a presynaptic  $\alpha_1$ -adrenoceptor-mediated mechanism<sup>31</sup>. This enhanced period of release may activate NMDA and/or metabotropic glutamate receptors (mGluRs) leading to a postsynaptic increase in synaptic strength. Although activation of NMDA receptors is crucial for hippocampal plasticity<sup>20</sup>, blockade of these receptors (with  $100$   $\mu$ M D-L-AP5) did not affect the ability of norepinephrine to increase quantal amplitude ( $1.25 \pm 0.05$ ,  $P < 0.01$ ,  $n = 5$ , **Fig. 4c**). Although the experiments in which postsynaptic inclusion of GDP- $\beta$ s and thapsigargin (above) would argue against a role for postsynaptic mGluRs, we directly tested for

**Figure 3** The enduring increase in mEPSC amplitude requires SNARE-dependent exocytosis, an increase in postsynaptic calcium and activation of PI3K. **(a)** Top: average mEPSCs before and after norepinephrine application with postsynaptic botulinum toxin C ( $5$   $\mu$ g/ml) to block SNARE-dependent exocytosis. Bottom: cumulative probability plot of mEPSC amplitudes ( $P > 0.05$ ) from the same cell. **(b)** Top: average mEPSCs before and after norepinephrine with postsynaptic EGTA ( $10$  mM) to chelate calcium. Bottom: cumulative fraction plot ( $P > 0.05$ ) from the same cell. **(c)** Top: average mEPSCs before and after norepinephrine with postsynaptic LY294002 ( $10$   $\mu$ M) to block PI3K activation. Bottom: cumulative fraction plot ( $P > 0.05$ ) from the same cell. Scale bars  $10$  pA,  $5$  ms.



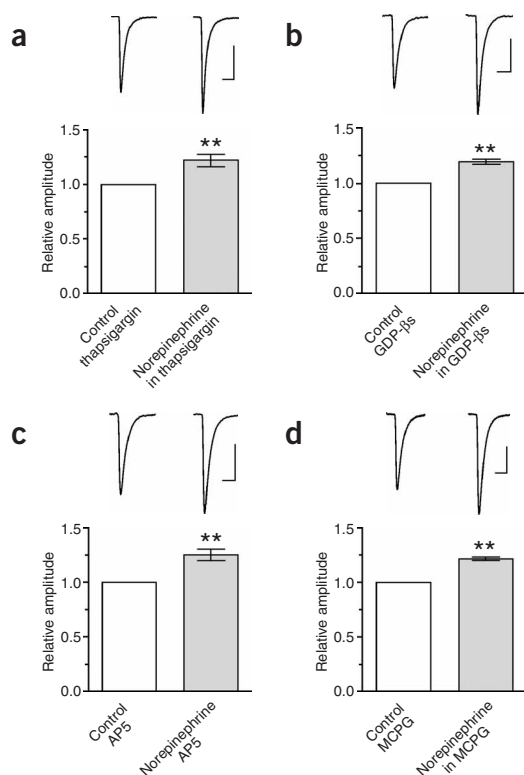


**Figure 4** The enduring increase in mEPSC amplitude does not involve postsynaptic  $\alpha_1$ -adrenoceptors or glutamate signaling. **(a)** Top: average mEPSCs before and after norepinephrine application with postsynaptic thapsigargin (5  $\mu$ M) to deplete calcium stores. Bottom: summary of effects of thapsigargin ( $1.22 \pm 0.05$ ,  $P < 0.01$ ,  $n = 8$ ). **(b)** Top: average mEPSCs before and after norepinephrine application with postsynaptic GDP- $\beta$ s (1 mM) to block G protein signaling. Bottom: summary of effects of GDP- $\beta$ s ( $1.19 \pm 0.02$ ,  $P < 0.01$ ,  $n = 6$ ). **(c)** Top: average mEPSCs before and after norepinephrine application with the NMDA receptor antagonist AP5 (100  $\mu$ M). Bottom: summary of effects of AP5 ( $1.25 \pm 0.05$ ,  $P < 0.01$ ,  $n = 5$ ). **(d)** Top: average mEPSCs before and after norepinephrine with the mGluR antagonist MCPG (200  $\mu$ M). Bottom: summary of effects of MCPG ( $1.21 \pm 0.01$ ,  $P < 0.01$ ,  $n = 5$ ). Scale bars: 10 pA, 5 ms. Error bars: s.e.m.

their contribution by applying norepinephrine in the presence of the group I mGluR antagonist MCPG (200  $\mu$ M). Under these conditions, norepinephrine still increased synaptic strength ( $1.21 \pm 0.01$ ,  $P < 0.01$ ,  $n = 5$ , **Fig. 4d**). Collectively, these observations argue against a role for postsynaptic  $\alpha_1$ -adrenoceptors, NMDA receptors or group I mGluRs in mediating the enduring increase in mEPSC amplitude.

#### P2X<sub>7</sub> receptor activation is necessary and sufficient

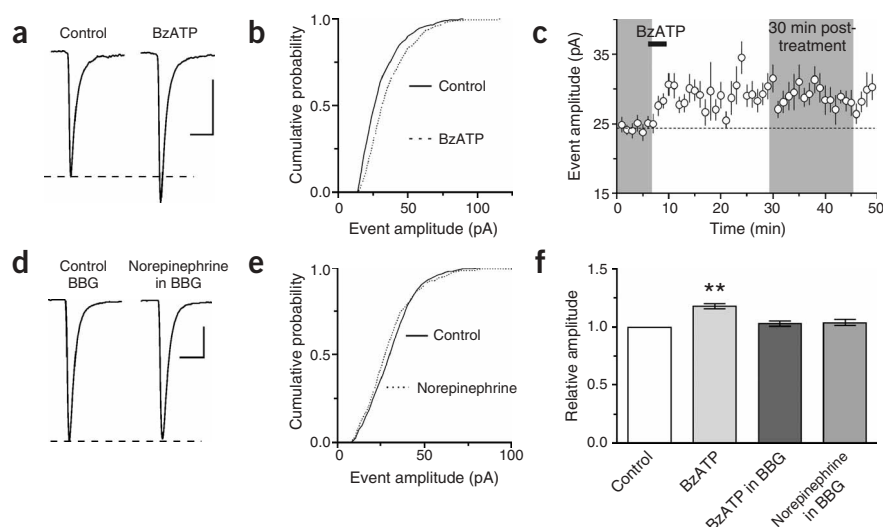
The excitatory effects of norepinephrine on MNC firing observed *in vivo* are attenuated by blockade of purinergic receptors<sup>21</sup>. We tested the hypothesis that direct activation of ATP-gated P2X receptors in our

slice preparation would effectively mimic the effects of norepinephrine on synaptic strength. Our experiments targeting postsynaptic G protein signaling argue against the metabotropic P2Y receptors, but MNCs possess a variety of functional P2X receptors capable of passing calcium<sup>12</sup>. We first tested ATP directly. Bath application of 30  $\mu$ M ATP elicited a sustained increase in mEPSC amplitude ( $1.15 \pm 0.02$ ,  $P < 0.05$ ,  $n = 7$ ). As ATP can be rapidly broken down by ectonucleotidases, this effect may be an underestimation. We repeated the experiment with BzATP, an analogue that is not readily degraded and can also activate several P2X channels, including P2X<sub>1</sub>, P2X<sub>3</sub> and P2X<sub>7</sub> (ref. 37). BzATP (30  $\mu$ M, 3 min) increased mEPSC amplitude ( $1.17 \pm 0.02$ ,  $P < 0.01$ ,  $n = 8$ , **Fig. 5a–c**). We next tested the hypothesis that activation of P2X<sub>7</sub> receptors was necessary for the norepinephrine-induced increase in synaptic strength. In the continuous presence of brilliant blue G (BBG, 1  $\mu$ M) a P2X receptor antagonist that blocks P2X<sub>7</sub> at the concentration used here<sup>37</sup>, norepinephrine failed to cause an enduring increase in mEPSC amplitude ( $1.04 \pm 0.02$ ,  $P > 0.05$ ,  $n = 5$ , **Fig. 5d–f**). BBG also blocked the increase in synaptic strength induced by BzATP ( $1.03 \pm 0.03$ ,  $P > 0.05$ ,  $n = 5$ , **Fig. 5f**). These data indicate that ATP-gated P2X<sub>7</sub> receptor activation is both necessary and sufficient for increasing mEPSC amplitude.

#### $\alpha_1$ -adrenoceptors are colocalized with a glial marker

Glial cells possess receptors for norepinephrine<sup>38</sup>, and in the PVN, a large fraction of noradrenergic terminals lack postsynaptic contacts<sup>23</sup>, leaving norepinephrine free to activate these cells. As the enduring enhancement of quantal amplitude is independent of glutamate

**Figure 5** Activation of P2X<sub>7</sub> receptors is necessary and sufficient for the expression of the enduring increase in mEPSC amplitude. **(a)** Average mEPSC traces from control condition and 30 min post-BzATP (30  $\mu$ M, 3 min). **(b)** Cumulative fraction plot of mEPSC amplitudes ( $P < 0.01$ ); same cell as **a**. **(c)** Running average of mEPSC amplitude in 1-min bins. **(d)** Average mEPSC traces from control condition and post-norepinephrine in the presence of the P2X antagonist BBG (1  $\mu$ M). **(e)** Cumulative fraction plot ( $P > 0.05$ ), same cell as **d**. **(f)** Summary: BzATP induces an enduring increase in mEPSC amplitude ( $1.17 \pm 0.02$ ,  $P < 0.01$ ,  $n = 8$ ), this effect is blocked by BBG ( $1.03 \pm 0.03$ ,  $P > 0.05$ ,  $n = 5$ ), and the enduring increase in mEPSC amplitude observed after norepinephrine is blocked with BBG ( $1.04 \pm 0.02$ ,  $P > 0.05$ ,  $n = 5$ ). Scale bars: 10 pA, 5 ms. Error bars: s.e.m.



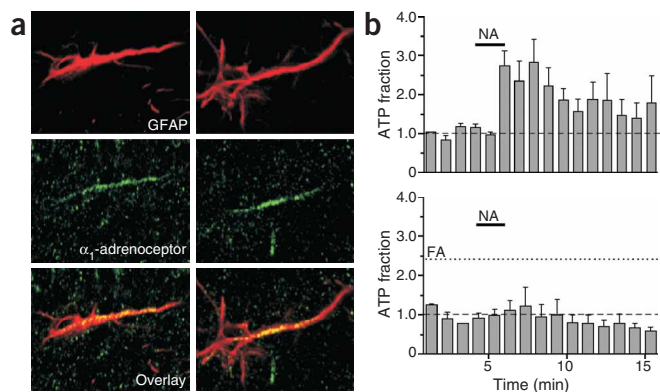


**Figure 6** Norepinephrine targets glial cells to release ATP. **(a)** Slice immunohistochemistry for the glial marker GFAP (top) and for the  $\alpha_1$ -adrenoceptor (middle). Overlaid confocal images show colocalization (bottom). Each picture comprises a series of stacked images, and each column is an example from a different rat. **(b)** Top: summary of relative increase in ATP release in response to norepinephrine (10–50  $\mu$ M) from cultured glial cells (peak ATP release:  $2.39 \pm 0.17$ ,  $P < 0.01$ ,  $n = 18$ ). Bottom: summary demonstrating that norepinephrine-induced release of ATP is blocked in the presence of the fluorocitric acid ( $1.02 \pm 0.07$ ,  $P > 0.05$ ,  $n = 7$ ). Data represent the pooled responses from four separate glial culture systems: pituitary, neonatal hypothalamus, hippocampus and neocortex. Error bars: s.e.m.

receptors and postsynaptic G protein signaling, yet requires the activation of  $\alpha_1$ -adrenoceptors, we tested the hypothesis that the observed effect in response to norepinephrine was secondary to the activation of glial cells. We first tested for the presence of  $\alpha_1$ -adrenoceptors on glial cells in PVN using immunohistochemical techniques. Astrocytes were identified with glial fibrillary acidic protein (GFAP) staining, and long astrocytic processes were clearly labeled in the PVN (Fig. 6a, top). In addition, a primary antibody directed against the  $\alpha_{1a}$ -adrenoceptor subunit resulted in both punctate staining and staining characterized by long thin sections (Fig. 6a, middle). Although it is clear that  $\alpha_1$ -adrenoceptors are not localized exclusively to glial cells, confocal images showed a strong colocalization between the signal for the  $\alpha_{1a}$ -antibody and GFAP in the glial processes (Fig. 6a, bottom).

#### Norepinephrine releases ATP from cultured glial cells

We next investigated whether norepinephrine would elicit the release of ATP from cultured glial cells. To test this directly we used a system of cultured pituitary cells. These glial cells engulf the neuropeptide-secreting terminals of the MNCs in the posterior pituitary and undergo

structural reorganization similar to that seen with SON and PVN glia in response to dehydration, parturition and lactation<sup>39</sup>. Using an ATP bioluminescence assay, we observed an increase in the ATP concentration in the surrounding saline in response to norepinephrine (10–50  $\mu$ M). We then confirmed the ubiquitous nature of this phenomenon in three separate culture systems in which glial cells were isolated from the neonatal hypothalamus, hippocampus or the neocortex. Again, in each of these preparations, norepinephrine robustly increased the concentration of ATP in the surrounding media. As the increases in extracellular ATP were qualitatively similar across cultures, the data were pooled. During the first five minutes after norepinephrine application, ATP levels increased  $2.39 \pm 0.17$ -fold over the control condition ( $P < 0.01$ ,  $n = 18$ , Fig. 6b, top).

We then used a pharmacological tool, fluorocitric acid (100  $\mu$ M), to examine whether the norepinephrine effect could be abated when the glial Krebs cycle was blocked<sup>40</sup>. Cultures were incubated for a minimum of 2 h in fluorocitric acid before norepinephrine was applied. Under these conditions, norepinephrine did not trigger the release of ATP ( $1.02 \pm 0.07$ ,  $P > 0.05$ ,  $n = 7$ , Fig. 6b, bottom).

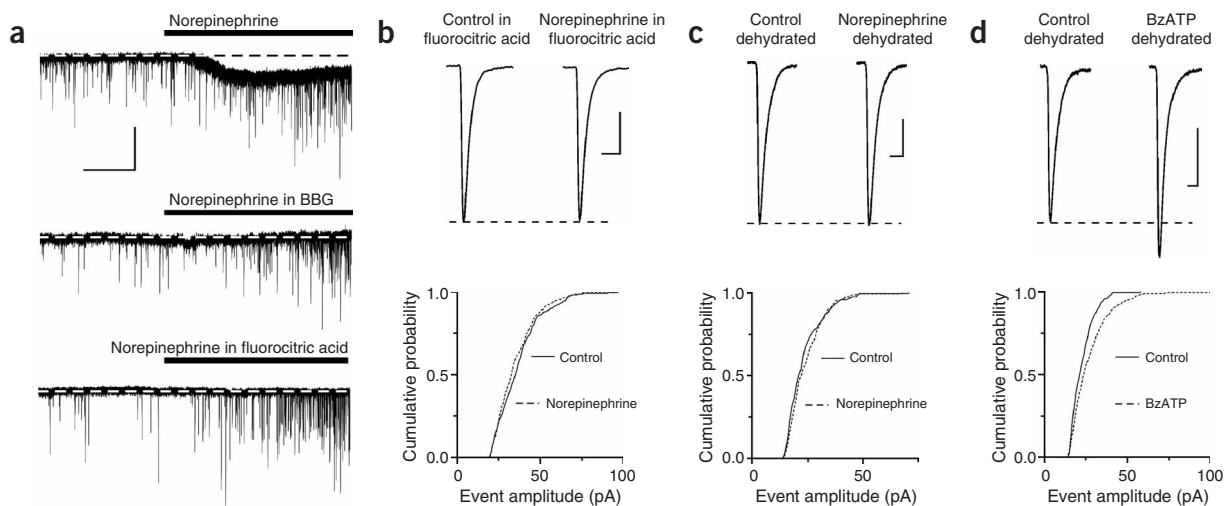


**Figure 7** Glial cells are necessary for the enduring increase in mEPSC amplitude triggered by  $\alpha_1$ -adrenoceptor activation. **(a)** Top: inward current at the onset of the norepinephrine effect ( $18.6 \pm 3.4$  pA,  $P < 0.01$ ,  $n = 8$ ). The inward current was blocked when P2X channels were blocked with BBG ( $2.3 \pm 3.6$  pA,  $P > 0.05$ ,  $n = 6$ ; middle) and when slices were incubated for > 2 h with fluorocitric acid ( $3.6 \pm 1.0$  pA,  $P > 0.05$ ,  $n = 6$ ; bottom). **(b)** Top: average mEPSC traces from control condition and post-norepinephrine treatment after fluorocitric acid incubation. Bottom: cumulative fraction plot of mEPSC amplitudes ( $P > 0.05$ ) from the same cell. **(c)** Top: average mEPSC traces from control condition and post-norepinephrine treatment after a 7- to 10-d dehydration protocol that elicits reduced glial coverage of synaptic contacts. Bottom: cumulative fraction plot of mEPSC amplitudes ( $P > 0.05$ ) from the same cell. **(d)** Top: average mEPSC traces from control condition and post-BzATP treatment in the dehydrated state. Bottom: cumulative fraction plot of mEPSC amplitudes ( $P < 0.01$ ) from the same cell. Scale bars: **a**: 40 pA, 30 s; **b,c,d**: 10 pA, 5 ms.

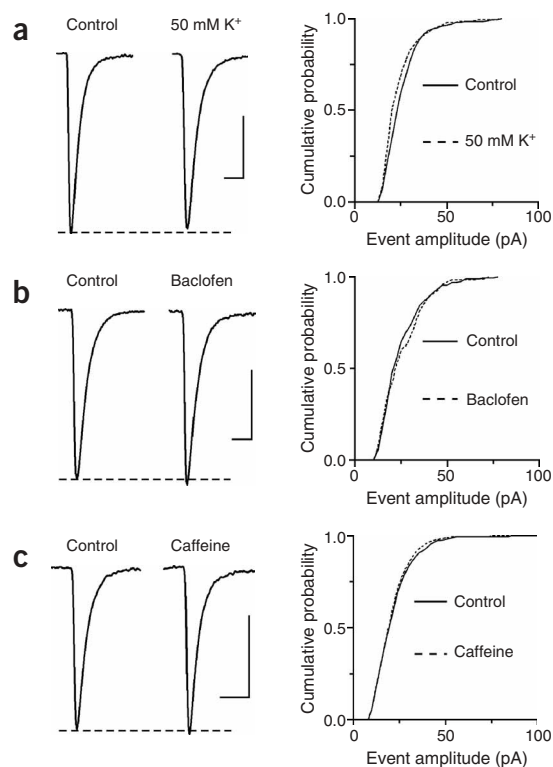


**Figure 8** A general rise in calcium in glial cells does not mimic the enduring increase in mEPSC amplitude observed in response to norepinephrine.

(a) Left: average mEPSC traces showing no change in current amplitude after the bath application of 50 mM K<sup>+</sup> in osmotically normal ACSF (2 min). Right: cumulative fraction plot of mEPSC amplitudes ( $P > 0.05$ ) from the same cell. (b) Left: average mEPSC traces showing that the GABA<sub>B</sub> receptor agonist baclofen (20 μM, 3 min) does not increase mEPSC amplitude. Right: cumulative fraction plot of mEPSC amplitudes ( $P > 0.05$ ) from the same cell. (c) Left: average mEPSC traces showing no change in current amplitude after bath application of caffeine (5 μM, 3 min). Right: cumulative fraction plot of mEPSC amplitudes ( $P > 0.05$ ) from the same cell. Scale bars: 10 pA, 5 ms.

### Glial cells are necessary for the norepinephrine effect

We next used several different tactics to determine whether the ATP responsible for the norepinephrine-induced plasticity in brain slices was derived from glia. First, we tested for the possibility that ATP, released from nerve terminals in our preparation, gates fast purinoreceptor-mediated synaptic transmission<sup>41</sup>. To maximize the likelihood of detecting ATP-mediated synaptic events, AMPA receptors were blocked (DNQX, 10 μM), and norepinephrine was applied. We did not detect any currents with kinetic features consistent with the rapid activation of ligand-gated ionotropic channels in response to synaptically released ATP<sup>41</sup> (data not shown). We next examined our data for a slower, more prolonged inward current that might be indicative of a neuronal response to diffuse activation of membrane receptors. Both norepinephrine and BzATP elicited a slow inward current that preceded the increase in mEPSC amplitude (norepinephrine:  $18.6 \pm 3.4$  pA,  $n = 8$ ; Fig. 7a, top; BzATP:  $8.8 \pm 1.5$  pA,  $n = 8$ ). Furthermore, the inward current induced by norepinephrine was abolished by BBG ( $2.3 \pm 3.6$  pA,  $n = 6$ ; Fig. 7a, middle), suggesting that this response is P2X<sub>7</sub> mediated. Notably, the transient increases in both frequency and amplitude elicited by norepinephrine were unaffected by BBG (Fig. 7a).

To test the hypothesis that ATP in the slice is derived from glial cells, we again used fluorocitric acid to inhibit the glial Krebs cycle<sup>40</sup>. Similar to the culture systems, slices were incubated for a minimum of 2 h in fluorocitric acid before norepinephrine treatment. Under these conditions, norepinephrine did not increase the amplitude of mEPSCs ( $0.98 \pm 0.02$ ,  $P > 0.05$ ,  $n = 6$ , Fig. 7b). Notably, the basal amplitude of mEPSCs from slices incubated in fluorocitric acid was not different from that in slices incubated in control solution (control:  $28.15 \pm 2.25$  pA; fluorocitric acid:  $27.10 \pm 2.40$  pA,  $P > 0.05$ ,  $n = 10$ ). We also did not observe an inward current in response to norepinephrine ( $3.6 \pm 1.0$  pA,  $P > 0.05$ ,  $n = 6$ , Fig. 7a, bottom), yet the transient increases in mEPSC frequency and amplitude at the commencement of norepinephrine application were unaltered.

Finally, we used a physiological tool to assess the putative contribution of glial cells to the norepinephrine-induced synaptic potentiation. Glial coverage of synapses in the magnocellular neurosecretory nuclei can be decreased markedly by physiological challenges, such as parturition, lactation and dehydration<sup>18,19</sup>. Such dynamic changes in the physical relationship between neurons and glial cells increase glutamate spillover and increase presynaptic autoinhibition<sup>42</sup>. To test the hypothesis that synaptic glial processes are necessary for the norepinephrine-induced synaptic strengthening, we used an established dehydration protocol to cause glial retraction from synaptic contacts<sup>43</sup>. In these experiments, norepinephrine did not cause an enduring increase in the mEPSC amplitude ( $1.04 \pm 0.02$ ,  $P > 0.05$ ,  $n = 12$ ; Fig. 7c). Finally, to confirm that this effect is due to the absence of glial investiture (and hence availability of ATP) and not due to changes in postsynaptic P2X receptor expression or signaling, we applied BzATP directly to these slices and observed that the enduring increase in mEPSC amplitude could still be induced ( $1.16 \pm 0.02$ ,  $P < 0.01$ ,  $n = 6$ ; Fig. 7d). It is important to note that in six additional cells, BzATP had no effect on amplitude. Taken together, these findings support the assertion that the norepinephrine-induced enduring increase in synaptic strength requires the release of ATP from surrounding glial cells.

Although the precise mechanism of ATP release from glial cells remains controversial, there is increasing support for the idea that the process may be calcium independent<sup>7,44,45</sup>. To examine whether the release of ATP from hypothalamic glial cells is consistent with these observations, we used several strategies to increase the calcium concentration in glia and assessed their impact on mEPSC amplitude. First, we bath applied 50 mM K<sup>+</sup> in iso-osmotic artificial cerebrospinal fluid (ACSF; 2 min)<sup>38</sup>. This resulted in a pronounced inward current as well as an increase in mEPSC frequency that washed out completely (data not shown) but did not elevate mEPSC amplitude ( $0.97 \pm 0.01$ ,  $P > 0.05$ ,  $n = 5$ ; Fig. 8a). Second, we applied the GABA<sub>B</sub> receptor agonist baclofen (20 μM, 3 min)<sup>2</sup> which also did not increase mEPSC amplitude ( $0.99 \pm 0.01$ ,  $P > 0.05$ ,  $n = 7$ ; Fig. 8b). A decrease in the frequency of mEPSCs, consistent with the activation of GABA<sub>B</sub> receptors on glutamatergic terminals, was always observed, indicating that baclofen was reaching its target (data not shown). Although mGluRs can also increase calcium in glia<sup>46</sup>, this receptor, like the α<sub>1</sub>-adrenoceptor, is G<sub>q</sub>-coupled and thus did not allow us to discriminate between the contribution of calcium from intracellular stores and that of other second messengers (such as diacylglycerol or IP<sub>3</sub>/IP<sub>4</sub>) in promoting the release of ATP. Instead, we applied caffeine (5 μM, 3 min), which liberates calcium from intracellular stores. Caffeine, however, did not increase mEPSC amplitude ( $1.01 \pm 0.06$ ,  $P > 0.05$ ,  $n = 5$ ; Fig. 8c). Finally, we either depleted intracellular calcium stores by incubating slices in thapsigargin (5 μM, 45 min) or blocked calcium release with a high dose of ryanodine (100 μM, 20 min) before testing with norepinephrine. These experimental manipulations did not block the norepinephrine-induced increase in mEPSC amplitude (thapsigargin

+ norepinephrine:  $1.22 \pm 0.06$ ,  $P < 0.01$ ,  $n = 8$ ; ryanodine + norepinephrine:  $1.21 \pm 0.04$ ,  $P < 0.01$ ,  $n = 5$ ). These results are consistent with previous demonstrations suggesting that ATP release from glial cells occurs through a calcium-independent mechanism<sup>7,44,45</sup>.

## DISCUSSION

The data presented here support the conclusion that ATP, released from glial cells in response to activation of  $\alpha_1$ -adrenoceptors, increases synaptic strength at glutamatergic synapses by promoting the postsynaptic insertion of AMPA receptors. Our findings further expand the role of glial cells in regulating the efficacy at excitatory synapses in the CNS<sup>1,3,4,42,47,48</sup>.

The assertion that glia are the source of the ATP is consistent with both anatomical findings describing catecholaminergic terminals that lack direct postsynaptic contacts<sup>23</sup> and physiological findings that norepinephrine can directly activate astrocytes<sup>38</sup>. Although it is clear that  $\alpha_1$ -adrenoceptors, in addition to being present on glial processes, are also present on non-GFAP-positive elements throughout the PVN, our inability to affect the expression of synaptic potentiation by either interfering with postsynaptic G protein function or depleting postsynaptic intracellular calcium stores argues against a direct postsynaptic action of norepinephrine. ATP may also be released in a vesicular fashion from presynaptic terminals in PVN. ATP-mediated synaptic currents have been reported in the CNS<sup>41</sup>, but we did not see any evidence for fast synaptic currents in the absence of glutamatergic signaling. We did, however, observe a slow, inward P2X<sub>7</sub>-mediated current in response to either norepinephrine or BzATP, which may be indicative of a slow increase in the concentration of a transmitter in the extracellular space, as might be predicted if ATP were released some distance from the postsynaptic cell. Although not on the same time scale, slow inward currents mediated by the activation of extrasynaptic NMDA receptors in response to glial glutamate have been recently described in hippocampal CA1 pyramidal neurons<sup>46</sup>. We were also able to block the increase in synaptic strength in response to norepinephrine by either pharmacologically compromising glial cells<sup>40</sup> or using physiological manipulations that decrease the astrocytic coverage of synapses in the magnocellular neurosecretory system<sup>18,43</sup>. Finally, we demonstrate that application of norepinephrine directly onto neuron-free glial cultures increases the release of ATP. The norepinephrine-driven ATP release from glial cells provides a mechanism by which glia can respond to, and exert influence over, synaptic activity. Glia are known to respond to norepinephrine with increases in intracellular calcium<sup>38</sup>. Whether an increase in intragial calcium can stimulate, or is even necessary for, ATP release is contentious. Both calcium-dependent<sup>49</sup> and calcium-independent<sup>7,44,45</sup> mechanisms have been described. We have found that increasing calcium either non-specifically (high K<sup>+</sup>) by activating a membrane-bound G protein-coupled receptor (baclofen) or by promoting release from intracellular stores (with caffeine) does not mimic the effects of norepinephrine on synaptic strength; this is most consistent with the idea that ATP release is not intimately linked to an increase in intragial calcium.

Our results also indicate that the key intracellular signaling molecules, postsynaptic calcium and PI3K<sup>14,20</sup>, that have been linked to the insertion of new AMPA receptors in other brain regions are conserved during the ATP-mediated increase in postsynaptic efficacy described here. Although the initial trigger for activation of this cascade in MNCs is different from that in a region such as the hippocampus, the ATP-gated P2X<sub>7</sub> receptor essentially serves as a surrogate for the NMDA receptor. The increase in mEPSC amplitude is blocked by buffering postsynaptic calcium with EGTA, interfering with PI3K signaling or by preventing vesicular fusion, all critical requirements for the insertion of

new AMPA receptors into the postsynaptic membrane<sup>14,20</sup>. Our findings also support previous reports of P2X<sub>7</sub> coupling to the PI3K/Akt pathway<sup>13</sup>. Although we cannot explicitly rule out the involvement of heteromeric P2X receptors or a contribution of P2Y receptors, our observations indicate that activation of the P2X<sub>7</sub> receptor alone is sufficient for the calcium entry and that PI3K activation is necessary for the enduring increase in mEPSC amplitude in our preparation.

In addition to advancing our understanding of the codependent interactions between glia and neurons, our findings also offer insights into a form of plasticity that may not be synapse specific (like LTP)<sup>20</sup>. Rather, it may be a new mechanism through which a single-point activation of interconnected glial networks may lead to changes in the synaptic strength of spatially distributed neuronal circuits and may contribute to the synchronization of firing activity in populations of cells that are not synaptically coupled<sup>46</sup>.

## METHODS

**Electrophysiology.** Hypothalamic coronal slices (300  $\mu$ m) containing PVN were prepared from male Sprague-Dawley rats (postnatal day (P) 21–28; Charles River). To promote retraction of glial cells, we used a dehydration protocol in which a solution of 2% NaCl was substituted for tap water for 7–10 d<sup>43</sup>. Animal use protocols were approved by the University of Calgary Animal Care and Use Committee. Animals were anesthetized (sodium pentobarbital 0.1 ml/100 g body weight) and decapitated, and brains were removed into ice-cold slicing solution for 3 min containing (in mM) NaCl 87, KCl 2.5, NaHCO<sub>3</sub> 25, CaCl<sub>2</sub> 0.5, MgCl<sub>2</sub> 7, NaH<sub>2</sub>PO<sub>4</sub> 1.25, glucose 25, sucrose 75, saturated with 95% O<sub>2</sub>/5% CO<sub>2</sub>. The brain was blocked and mounted on a vibrating slicer (Leica Instruments) submerged in ice-cold slicing solution. Slices were incubated at 32.5 °C in ACSF containing (in mM) NaCl 126, KCl 2.5, NaHCO<sub>3</sub> 26, CaCl<sub>2</sub> 2, MgCl<sub>2</sub> 2, NaH<sub>2</sub>PO<sub>4</sub> 1.25, glucose 10, saturated with 95% O<sub>2</sub>/5% CO<sub>2</sub>, for a minimum of 60 min. Using an upright microscope (Zeiss Axioskop II FS Plus) fitted with infrared differential interference contrast, whole-cell recordings were obtained from magnocellular PVN neurons (as confirmed by their distinct morphology and electrophysiological characteristics). All experimental recordings were obtained at 32.5 °C in voltage-clamp mode and were accepted barring changes in access resistance of >15%. The intracellular solution contained (in mM) potassium gluconate 123, MgCl<sub>2</sub> 2, NaCl 8, potassium EGTA 1, potassium ATP 4, and sodium GTP 0.3 buffered with KHCO<sub>3</sub> 16. In experiments in which drugs were introduced to the postsynaptic cell through the patch electrode, a minimum of 20 min was allowed for intracellular diffusion. For experiments with thapsigargin, a minimum diffusion time of 30 min was given. When GDP- $\beta$ s was included in the internal solution, GTP was removed. The perfusate always contained picrotoxin (100  $\mu$ M) to block GABA<sub>A</sub> channels and tetrodotoxin (1  $\mu$ M) to block voltage-gated Na<sup>+</sup> channels. Cells were held at –80 mV to increase ionic driving force and to block the contribution of NMDA receptors to the synaptic response. In experiments using focal administration of AMPA (3-ms pulse, 100  $\mu$ M, 25 psi), puffs were performed once every minute in the control, norepinephrine and wash conditions using a Picospritzer 2 (General Valve Corporation). The spritzing tips (resistance 3–6 m $\Omega$ ) were placed directly over the soma of the patched cell. The response elicited was validated with 5  $\mu$ M DNQX, which completely blocked the response ( $n = 3$ ).

**Immunohistochemistry.** Male Sprague-Dawley rats (P21–28; Charles River) were anesthetized with sodium pentobarbital and perfused transcardially with cold phosphate buffered saline (PBS) followed by 4% paraformaldehyde. The brains were harvested and post-fixed in 4% paraformaldehyde overnight and then cryoprotected in 30% sucrose for another 24 h. Sections were cut on a cryostat to 30  $\mu$ m and floated in PBS. The sections were washed in 0.2% Tween-20 in PBS for 10 min, followed by 30 min in 1% hydrogen peroxide to clear excess peroxidases. Sections were then washed three times before blocking (3% donkey serum, 0.2% Tween-20 and 2% dimethylsulfoxide (DMSO) in PBS) for 1 h. Subsequently, sections were incubated at 20–22 °C for 24 h with an affinity-purified rabbit polyclonal antibody against the  $\alpha_{1a}$ -adrenoceptor (Sigma, 1:250 in blocking buffer) followed by three washes

(0.2% Tween-20, 2% DMSO in PBS) before incubation for two hours with Alexa Fluor 488 donkey anti-rabbit (Molecular Probes, 1:250 in blocking buffer). Sections were washed again three times (0.2% Tween-20, 2% DMSO in PBS) followed by a second 24-h incubation with a mouse monoclonal GFAP antibody conjugated with Cy3 (Sigma, 1:500 in blocking buffer). Sections were subsequently washed and mounted onto chrom alum-coated slides, coverslipped with Vectashield (Vector Labs) and visualized on a confocal microscope (Olympus, BX-51). Each image in **Figure 6** comprises 12 sequential 1- $\mu$ m plane images stacked together. Colocalization of GFAP and  $\alpha_1$ -adrenoceptor was also verified on a single plane occurring within the uppermost section of the glial process.

**Glial cell culture.** Brains of two-day-old neonatal Wistar rats were removed after decapitation and were dissected using a dissecting microscope to separate hippocampus and cortex. These were separately mashed through an 80- $\mu$ m Nitex mesh using a metal rod under aseptic conditions, as described<sup>50</sup>. All steps were carried out on ice. The collected cell suspension was cultured in 35-mm culture dishes in DMEM medium (Invitrogen) containing 10% fetal calf serum and was maintained at 37 °C in a humidified atmosphere containing 5% CO<sub>2</sub>. The medium was changed every 3–4 d. The cultures were used for the ATP assay after 10 d. For the pituitary culture, posterior pituitaries were separated from decapitated adult Long-Evans rats using a dissecting microscope. The tissue was cut into eight pieces, each of which was attached to the bottom of a 35-mm culture dish in a fibrin clot and cultured under the conditions described above. The cells were used for the ATP assay after 14 d. For the ATP assay, the cell medium was replaced with physiological saline containing (in mM) NaCl 120, KCl 4, MgCl<sub>2</sub> 1.2, glucose 10, CaCl<sub>2</sub> 2, HEPES 10, pH 7.35. During the experiment, the saline was replaced every 2 min and an aliquot was used to measure ATP using an ATP bioluminescent assay kit (Sigma) and a 1251 luminometer (LKB Wallac) at room temperature. The light output was measured 1 min after the beginning of the luciferase reaction. During the two exchanges indicated, the saline also contained 10–50  $\mu$ M norepinephrine.

**Data collection and statistics.** Signals were amplified with the Multiclamp 700A amplifier (Axon Instruments), low-pass filtered at 1 kHz and digitized at 10 kHz using the Digidata 1322 (Axon Instruments). Data were collected (pClamp, Axon Instruments) and stored on computer for offline analysis using software designed to detect miniature synaptic events using a variable threshold (MiniAnalysis, Synaptosoft). The amplitude of mEPSCs was obtained during the control condition and 30 min after the cessation of norepinephrine or BzATP, where a minimum of 5 min (up to 10 min) of recording was taken for analysis. In each experiment, the change in mEPSC amplitude was assessed as a fraction of one. All cells in a given experimental set were averaged and are presented as mean  $\pm$  s.e.m. Statistical analyses were performed using a two-tailed Student's *t*-test when comparing two groups, an analysis of variance (ANOVA) with a post-hoc Newman-Keuls test for comparisons across multiple groups and a Kolmogorov-Smirnov test for comparing two cumulative distributions.  $P < 0.05$  was accepted as statistically significant (\*,  $P < 0.05$ ; \*\*,  $P < 0.01$ ).

**Peak-scaled non-stationary noise analysis (PSNA).** The stochastic gating properties of AMPA receptors were assessed with PSNA using Synaptosoft Minianalysis software. In brief, 100–200 mEPSCs were selected with rise times  $< 1$  ms, aligned at steepest rise and then averaged. The mean mEPSC waveform was scaled to each individual mEPSC and subtracted to obtain the difference decay current. The variance was calculated between all difference currents, and a correction for post-mEPSC baseline variance was made. A parabolic relationship was obtained from the decay variance versus mean decay current plot and a regression line was fit to the first 50% of the data points back-calculated from the end-of-decay baseline. The slope of this relationship represents the weighted mean single-channel current, and the conductance is calculated from Ohm's law,  $g = i / E - E_x$ , where  $i$  represents the unitary current, and  $E - E_x$  is the driving force (80 mV).

**Drugs.** Norepinephrine (1-[3,4-dihydroxyphenyl]-2-aminoethanol), phenylephrine ((R)-(-)-1-(3-hydroxyphenyl)-2-methylaminoethanol hydrochloride), prazosin (1-[4-amino-6,7-dimethoxy-2-quinazolinyl]-4-[2-furanylcarbonyl]-piperazine), DNQX (6,7-dinitroquinoxaline-2,3(1H,4H)-dione), AMPA,

LY294002 (2-(4-morpholinyl)-8-phenyl-1(4H)-benzopyran-4-one hydrochloride), wortmannin, BBG, BzATP (2'-3'-o-(4-benzoylbenzoyl)adenosine 5'-triphosphate triethylammonium salt), ATP, picrotoxin, GDP- $\beta$ s (guanosine 5'-[b-thio]diphosphate trithium salt), MCPG ( $\alpha$ -methyl-(4-carboxyphenyl)-glycine)), fluorocitric acid (D,L-fluorocitric acid, barium salt), baclofen (( $\pm$ )-b-(aminomethyl)-4-chlorobenzeneprapanoic acid), thapsigargin and ryanodine (ryanodol 3-(1H-pyrrole-2-carboxylate), *Ryania speciosa*) were purchased from Sigma. Tetrodotoxin was purchased from Alomone Labs. Botulinum toxin C was purchased from Calbiochem. Picrotoxin, wortmannin and LY294002 were dissolved in DMSO (final concentration  $< 0.1\%$ ). Prazosin was dissolved in methanol (final bath concentration  $< 0.05\%$ ). MCPG was dissolved in 0.1 M NaOH. Fluorocitric acid was dissolved in ACSF with 15 min of sonication.

#### ACKNOWLEDGMENTS

We thank C. Sank for technical assistance and for conducting the immunohistochemistry experiments. We are also grateful to Q. Pittman for assistance with the dehydration protocol and for comments on an earlier version of the manuscript and to S. Oliet and B. MacVicar for helpful discussions. This work was supported by operating grants to J.S.B. from the Canadian Institutes of Health Research (CIHR) and T.E.F. from the Heart and Stroke Foundation of Saskatchewan. G.R.J.G. is supported by a studentship from the Natural Sciences and Engineering Research Council. J.S.B. is a CIHR New Investigator and an Alberta Heritage Foundation for Medical Research Scholar. T.E.F. is a CIHR/Regional Partnership Program New Investigator.

#### COMPETING INTERESTS STATEMENT

The authors declare that they have no competing financial interests.

Received 24 May; accepted 9 June 2005

Published online at <http://www.nature.com/natureneuroscience/>

- Parpura, V. *et al.* Glutamate-mediated astrocyte-neuron signalling. *Nature* **369**, 744–747 (1994).
- Kang, J., Jiang, L., Goldman, S.A. & Nedergaard, M. Astrocyte-mediated potentiation of inhibitory synaptic transmission. *Nat. Neurosci.* **1**, 683–692 (1998).
- Zhang, J.M. *et al.* ATP released by astrocytes mediates glutamatergic activity-dependent heterosynaptic suppression. *Neuron* **40**, 971–982 (2003).
- Beattie, E.C. *et al.* Control of synaptic strength by glial TNF $\alpha$ . *Science* **295**, 2282–2285 (2002).
- Robitaille, R. Modulation of synaptic efficacy and synaptic depression by glial cells at the frog neuromuscular junction. *Neuron* **21**, 847–855 (1998).
- Guthrie, P.B. *et al.* ATP released from astrocytes mediates glial calcium waves. *J. Neurosci.* **19**, 520–528 (1999).
- Wang, Z., Haydon, P.G. & Yeu, E.S. Direct observation of calcium-independent intercellular ATP signaling in astrocytes. *Anal. Chem.* **72**, 2001–2007 (2000).
- Cotrino, M.L., Lin, J.H., Lopez-Garcia, J.C., Naus, C.C. & Nedergaard, M. ATP-mediated glial signaling. *J. Neurosci.* **20**, 2835–2844 (2000).
- Khakh, B.S. Molecular physiology of P2X receptors and ATP signalling at synapses. *Nat. Rev. Neurosci.* **2**, 165–174 (2001).
- Shigetomi, E. & Kato, F. Action potential-independent release of glutamate by Ca<sup>2+</sup> entry through presynaptic P2X receptors elicits postsynaptic firing in the brainstem autonomic network. *J. Neurosci.* **24**, 3125–3135 (2004).
- Armstrong, J.N., Brust, T.B., Lewis, R.G. & MacVicar, B.A. Activation of presynaptic P2X7-like receptors depresses mossy fiber-CA3 synaptic transmission through p38 mitogen-activated protein kinase. *J. Neurosci.* **22**, 5938–5945 (2002).
- Shibuya, I. *et al.* Evidence that multiple P2X purinoceptors are functionally expressed in rat supraoptic neurons. *J. Physiol. (Lond.)* **514**, 351–367 (1999).
- Jacques-Silva, M.C. *et al.* P2X7 receptors stimulate AKT phosphorylation in astrocytes. *Br. J. Pharmacol.* **141**, 1106–1117 (2004).
- Man, H.Y. *et al.* Activation of PI3-kinase is required for AMPA receptor insertion during LTP of mEPSCs in cultured hippocampal neurons. *Neuron* **38**, 611–624 (2003).
- Sanna, P.P. *et al.* Phosphatidylinositol 3-kinase is required for the expression but not for the induction or the maintenance of long-term potentiation in the hippocampal CA1 region. *J. Neurosci.* **22**, 3359–3365 (2002).
- Raymond, C.R., Redman, S.J. & Crouch, M.F. The phosphoinositide 3-kinase and p70 S6 kinase regulate long-term potentiation in hippocampal neurons. *Neuroscience* **109**, 531–536 (2002).
- Lin, C.H. *et al.* A role for the PI-3 kinase signaling pathway in fear conditioning and synaptic plasticity in the amygdala. *Neuron* **31**, 841–851 (2001).
- Tweedle, C.D. & Hatton, G.I. Ultrastructural changes in rat hypothalamic neurosecretory cells and their associated glia during minimal dehydration and rehydration. *Cell Tissue Res.* **181**, 59–72 (1977).
- Theodosios, D.T. & Poulain, D.A. Activity-dependent neuronal-glial and synaptic plasticity in the adult mammalian hypothalamus. *Neuroscience* **57**, 501–535 (1993).
- Malinow, R. & Malenka, R.C. AMPA receptor trafficking and synaptic plasticity. *Annu. Rev. Neurosci.* **25**, 103–126 (2002).
- Day, T.A., Sibbald, J.R. & Khanna, S. ATP mediates an excitatory noradrenergic neuron input to supraoptic vasopressin cells. *Brain Res.* **607**, 341–344 (1993).

22. Kapoor, J.R. & Sladek, C.D. Purinergic and adrenergic agonists synergize in stimulating vasopressin and oxytocin release. *J. Neurosci.* **20**, 8868–8875 (2000).
23. Sawyer, C.H. & Clifton, D.K. Aminergic innervation of the hypothalamus. *Fed. Proc.* **39**, 2889–2895 (1980).
24. Carter, A.G. & Regehr, W.G. Quantal events shape cerebellar interneuron firing. *Nat. Neurosci.* **5**, 1309–1318 (2002).
25. Sharma, G. & Vijayaraghavan, S. Modulation of presynaptic store calcium induces release of glutamate and postsynaptic firing. *Neuron* **38**, 929–939 (2003).
26. Zucker, R.S. Can a synaptic signal arise from noise? *Neuron* **38**, 845–846 (2003).
27. Kombian, S.B., Hirasawa, M., Mougnot, D., Chen, X. & Pittman, Q.J. Short-term potentiation of miniature excitatory synaptic currents causes excitation of supraoptic neurons. *J. Neurophysiol.* **83**, 2542–2553 (2000).
28. Armstrong, W.E., Gallagher, M.J. & Sladek, C.D. Noradrenergic stimulation of supraoptic neuronal activity and vasopressin release in vitro: mediation by an alpha 1-receptor. *Brain Res.* **365**, 192–197 (1986).
29. Randle, J.C., Bourque, C.W. & Renaud, L.P. Alpha 1-adrenergic receptor activation depolarizes rat supraoptic neurosecretory neurons in vitro. *Am. J. Physiol.* **251**, R569–R574 (1986).
30. Daftary, S.S., Boudaba, C., Szabo, K. & Tasker, J.G. Noradrenergic excitation of magnocellular neurons in the rat hypothalamic paraventricular nucleus via intranuclear glutamatergic circuits. *J. Neurosci.* **18**, 10619–10628 (1998).
31. Gordon, G.R. & Bains, J.S. Priming of excitatory synapses by alpha1 adrenoceptor-mediated inhibition of group III metabotropic glutamate receptors. *J. Neurosci.* **23**, 6223–6231 (2003).
32. Traynelis, S.F., Silver, R.A. & Cull-Candy, S.G. Estimated conductance of glutamate receptor channels activated during EPSCs at the cerebellar mossy fiber-granule cell synapse. *Neuron* **11**, 279–289 (1993).
33. Benke, T.A., Luthi, A., Isaac, J.T. & Collingridge, G.L. Modulation of AMPA receptor unitary conductance by synaptic activity. *Nature* **393**, 793–797 (1998).
34. Stern, J.E., Galarreta, M., Foehring, R.C., Hestrin, S. & Armstrong, W.E. Differences in the properties of ionotropic glutamate synaptic currents in oxytocin and vasopressin neuroendocrine neurons. *J. Neurosci.* **19**, 3367–3375 (1999).
35. O'Connor, V. *et al.* Disruption of syntaxin-mediated protein interactions blocks neurotransmitter secretion. *Proc. Natl. Acad. Sci. USA* **94**, 12186–12191 (1997).
36. Di, S., Malcher-Lopes, R., Halmos, K.C. & Tasker, J.G. Nongenomic glucocorticoid inhibition via endocannabinoid release in the hypothalamus: a fast feedback mechanism. *J. Neurosci.* **23**, 4850–4857 (2003).
37. North, R.A. Molecular physiology of P2X receptors. *Physiol. Rev.* **82**, 1013–1067 (2002).
38. Duffy, S. & MacVicar, B.A. Adrenergic calcium signaling in astrocyte networks within the hippocampal slice. *J. Neurosci.* **15**, 5535–5550 (1995).
39. Tweedle, C.D. & Hatton, G.I. Morphological adaptability at neurosecretory axonal endings on the neurovascular contact zone of the rat neurohypophysis. *Neuroscience* **20**, 241–246 (1987).
40. Clarke, D.D. Fluoroacetate and fluorocitrate: mechanism of action. *Neurochem. Res.* **16**, 1055–1058 (1991).
41. Edwards, F.A., Gibb, A.J. & Colquhoun, D. ATP receptor-mediated synaptic currents in the central nervous system. *Nature* **359**, 144–147 (1992).
42. Oliet, S.H., Piet, R. & Poulain, D.A. Control of glutamate clearance and synaptic efficacy by glial coverage of neurons. *Science* **292**, 923–926 (2001).
43. Miyata, S., Nakashima, T. & Kiyohara, T. Structural dynamics of neural plasticity in the supraoptic nucleus of the rat hypothalamus during dehydration and rehydration. *Brain Res. Bull.* **34**, 169–175 (1994).
44. Leybaert, L., Paemeleire, K., Strahonja, A. & Sanderson, M.J. Inositol-trisphosphate-dependent intercellular calcium signaling in and between astrocytes and endothelial cells. *Glia* **24**, 398–407 (1998).
45. Anderson, C.M., Bergher, J.P. & Swanson, R.A. ATP-induced ATP release from astrocytes. *J. Neurochem.* **88**, 246–256 (2004).
46. Fellin, T. *et al.* Neuronal synchrony mediated by astrocytic glutamate through activation of extrasynaptic NMDA receptors. *Neuron* **43**, 729–743 (2004).
47. Araque, A., Parpura, V., Sanzgiri, R.P. & Haydon, P.G. Glutamate-dependent astrocyte modulation of synaptic transmission between cultured hippocampal neurons. *Eur. J. Neurosci.* **10**, 2129–2142 (1998).
48. Bezzi, P. & Volterra, A. A neuron-glia signalling network in the active brain. *Curr. Opin. Neurobiol.* **11**, 387–394 (2001).
49. Coco, S. *et al.* Storage and release of ATP from astrocytes in culture. *J. Biol. Chem.* **278**, 1354–1362 (2003).
50. Bekar, L.K. *et al.* Complex expression and localization of inactivating Kv channels in cultured hippocampal astrocytes. *J. Neurophysiol.* **93**, 1699–1709 (2005).